Paper No. 1665. (quote when citing this article)
Eleventh World Conference on Earthquake Engineering
ISBN: 0 08 042822 3

SLIDING ANALYSIS OF A SOFTLY INSTALLED OFFSHORE STRUCTURE COUPLED WITH INTERIOR AND EXTERIOR FLUID MOTION DUE TO EARTHQUAKE

Y. TANAKA*, A. SULEKH** and T. TSUKA**

* Technology Research Center, Taisei Corporation, Yokohama, 245, Japan
** Civil Engineering Design Dept., Taisei Corporation, Tokyo, 163, Japan

ABSTRACT

A numerical sliding simulation method of a softly installed offshore structure with multiple liquid storage tanks has been developed considering the coupled interaction between swaying motion of the rigid structure and both interior and exterior fluid hydrodynamic motion. Laboratory shaking table experiment has been conducted to verify the proposed numerical model. The effects of both interior and exterior fluid hydrodynamic interaction on the sliding behavior of the softly installed structure are investigated through our numerical implementation as well as vibration model tests. Hydrodynamic restoring forces of both interior and exterior fluid play an important role in sliding response of the softly installed offshore structure.

KEY WORDS

Softly installed offshore structure, Sliding response analysis, Sloshing of liquid storage tank, Hydrodynamic interaction of interior and exterior fluid motion, Boundary element method

INTRODUCTION

A softly installed offshore structure is defined as a sort of fixed type offshore structure whose ballast weight is lighter than a gravity type offshore structure; therefore, the space for ballast weight can be utilized for liquid storage tanks or plant utilities. The design concept of this kind of structure is that it is not allowed to slide for wave forces but is allowed to slide for strong earthquakes. One of the other main features is that it can be installed even on poor soil conditions without any particular soil improvements because of low contact pressure on the ground due to buoyancy. It has been proved by our case study that this structure has several advantages for an oil storage concrete platform, a liquid storage loading platform or a large offshore concrete island for coal combustion electric power plants; such as economical construction, short site construction period and smaller earthquake damage by allowing to slide. From the design point of view, one of the most important techniques for such structures is to precisely calculate the sliding response under severe earthquake condition. An experimental study of the hydrodynamic interaction between a sliding rigid body surrounded by exterior fluid and hydrodynamic restoring forces has been conducted by Uwabe and Higaki (1984) using a shaking table equipped in the wave basin. Fujii *et al.* (1986) have experimentally and theoretically investigated the interaction between the sliding response of a rigid body and the ground motion. Recently, Williams (1991) obtained a solution for axisymmetric intake and outlet towers fixed on the ground in which the influence of both interior and exterior compressive fluid was considered; appropriate Green's function led to a pair of coupled line-integral equations. Hitherto, any theoretical studies of hydrodynamic effects of both interior and exterior fluid on the sliding behavior of the softly installed offshore structure have not been carried out yet.

The hydrodynamic motions of both interior and exterior fluid are expressed in terms of velocity potential which is coupled with the sliding motion of the structure. The plural liquid storage tanks are modeled as several fluid domains inside the structure. The sea water surrounding the structure is modeled as semi-infinite fluid domain and/or finite fluid domain. The sliding response is fundamentally nonlinear behavior, therefore it

is numerically solved in time domain by Newmark's integration scheme. The velocity potential coupled with the dynamic motion of the structure is solved by Boundary Element Method. A numerical scheme for absorption of all outgoing waves at an open boundary in the exterior semi-infinite fluid domain has been developed based on an extension of the Orlanski boundary condition. Laboratory shaking table experiment has been carried out to verify the theoretical model focusing on the interaction between the sliding motion of the rigid body and the hydrodynamic sloshing motion of interior fluid. The parametric study changing the width of the divided intervals of the liquid storage tank, suggests that we can control the sliding displacement by adjusting the proper divided interval of the walls.

MATHEMATICAL FORMULATION

Boundary-value Problem

A two-dimensional softly installed structure with arbitrary number (N) of interior liquid storage tanks is surrounded by either semi-infinite water domain or finite water domain as shown in Fig. 1a. The ground is subjected to horizontal motion with acceleration amplitude $\ddot{Y}$. Both interior and exterior fluid is assumed to be invisid and incompressible and the flow to be irrotational. The fluid motion for each domain can then be described by a velocity potential $\Phi(x,z,t)$. Tanaka and Hudspeth (1988) investigated using their analytical solution that the water compressibility is important to precisely evaluate the hydrodynamic restoring force as well as the dynamic response of a flexible cylindrical structure due to horizontal ground acceleration, when the non-dimensional frequency Ω ($=2h\omega/\pi c$, where h is water depth, ω is angular frequency of ground motion, and c is acoustic speed in water) is greater than 0.7~0.8. The water depth for this softly installed structure such as a liquid storage loading platform is at most 20 m. The non-dimensional frequency Ω becomes therefore 0.028~0.56 for the condition that the input earthquake frequencies are set 0.5~10 Hz; thus, the water compressibility can be neglected in this numerical model. The governing equations to be solved are then Laplace equations for each interior (i=1,2,....,N) domain and exterior (i=c,o) domain, given by

$$\nabla^2\Phi_i = 0 \qquad \text{in } \Gamma_i \quad ; \ i = 1,2,....,N,c,o \tag{1}$$

where ∇^2 denotes the two-dimensional Laplace operator. If the horizontal motions of the ground and the rigid storage tank are defined as shown in Fig. 1b, the equation of motion of the sliding rigid body is given by

$$M(\ddot{Y} + \ddot{U}) = -\,\mathrm{sgn}(\dot{U})\mu_d W' - F \tag{2}$$

where M is the total mass of rigid body and interior fluid, X is the absolute displacement of the rigid body, Y is the absolute displacement of the ground, U is the relative displacement of the rigid body relative to the ground motion, F is the horizontal hydrodynamic restoring forces due to both interior and exterior fluid, μ_d is the dynamic friction coefficient and W' is the weight of the rigid body in water. The boundary conditions on the free surface S_{fi} (i=1,2,....,N,c,o) of both interior and exterior domains are given by

$$\frac{\partial\Phi_i}{\partial n} = -\frac{1}{g}\frac{\partial^2\Phi_i}{\partial t^2} \qquad \text{on } S_{fi} \quad ; \ i = 1,2,....,N,c,o \tag{3}$$

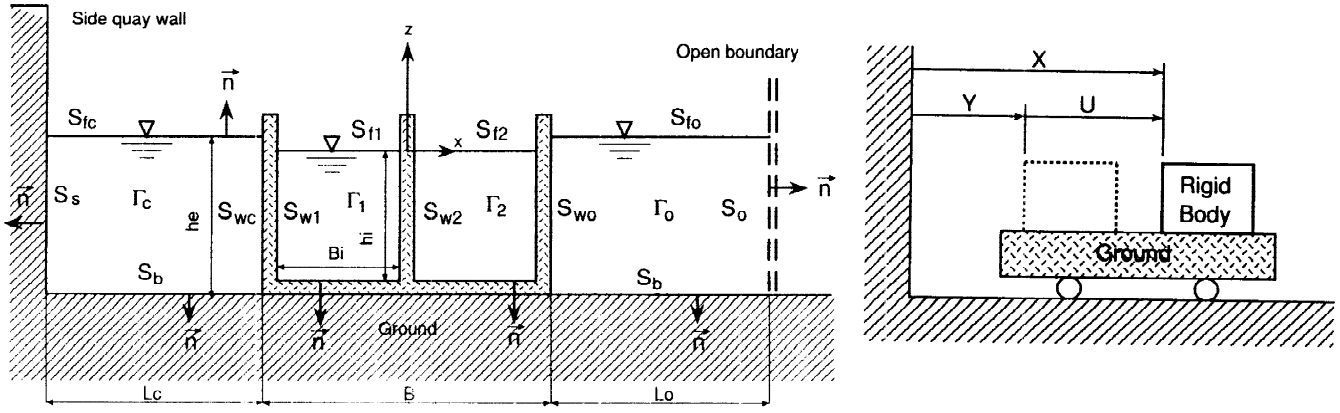

Fig. 1 Definition sketch of a) boundary-value problem and b) rigid body motion

where g is acceleration due to gravity. The kinematic boundary conditions on both interior and exterior body surface S_{wi}, on the sea bed S_b and on the side quay wall S_s are expressed, respectively

$$\frac{\partial \Phi_i}{\partial n} = \dot{X} n_x \quad \text{on } S_{wi}, i = 1,2,..,N,c,o \quad ; \quad \frac{\partial \Phi_i}{\partial n} = 0 \quad \text{on } S_b, i = c,o \quad ; \quad \frac{\partial \Phi_c}{\partial n} = \dot{Y} n_x \quad \text{on } S_s \tag{4}$$

where n is unit normal pointing away from fluid domain and n_x denotes the directional cosine with respect to the x axis. Finally it is necessary to introduce an artificial boundary to limit the domain of computation which ensure an unique solution. The Sommerfelt radiation condition on the open boundary S_o can be written as

$$\frac{\partial \Phi_o}{\partial n} = \frac{1}{C}\frac{\partial \Phi_o}{\partial t} \qquad \text{on } S_o \tag{5}$$

where C is the phase velocity and this condition applied in the time domain is often known as the Orlanski condition. Orlanski (1976) suggested that the phase velocity, instead of being a constant value, should be numerically determined from neighboring grid points.

The sliding response of the rigid body with liquid storage tanks due to the ground excitation indicates not only non-stationary state but also nonlinear behavior, thus it is necessary to solve the velocity potential as well as the sliding response in time domain as a boundary-value problem satisfying Eqs. (1) to (5). Applying Newmark's integration scheme to the time dependent velocity potential $\Phi(x,z,t)$, the following equations are obtained.

$$\Phi(t+1) = \Phi(t) + \Delta t\,\dot{\Phi}(t) + (\frac{1}{2} - \beta_2)\Delta t^2 \ddot{\Phi}(t) + \beta_2 \Delta t^2 \ddot{\Phi}(t+1) \tag{6}$$

$$\dot{\Phi}(t+1) = \dot{\Phi}(t) + (1 - \beta_1)\Delta t\,\ddot{\Phi}(t) + \beta_1 \Delta t\,\ddot{\Phi}(t+1) \tag{7}$$

where β_1 and β_2 are the parameters related to the integration accuracy and the integration stability, respectively, and Δt is the simulation time step. In order to apply the boundary-value problem to the Boundary Element Method, the normal derivative of the velocity potential at the time of (t+1) in the boundary conditions given by Eqs. (3), (4) and (5) should be expressed in terms of the velocity potential $\Phi(t+1)$. Substituting $\ddot{\Phi}(t+1)$ which is obtained from Eq. (6) into Eq. (3), the normal derivative of the velocity potential can be expressed in terms of the velocity potential $\Phi(t+1)$.

$$\frac{\partial \Phi_i(t+1)}{\partial n} = -\frac{1}{g\beta_2 \Delta t^2}\left[\Phi_i(t+1) - A_i(t)\right] \qquad \text{where} \qquad A_i(t) = \Phi_i(t) + \Delta t\,\dot{\Phi}_i(t) + (\frac{1}{2} - \beta_2)\Delta t^2 \ddot{\Phi}_i(t) \tag{8}$$

Let us consider the kinematic boundary conditions on both interior and exterior body surfaces at the time of (t+1) which should satisfy the equation of motion of the rigid body shown in Eq. (2). When the rigid body does not slide, the absolute velocity of the rigid body is equal to that of the ground; therefore the normal velocity of the body is given by

$$\frac{\partial \Phi_i(t+1)}{\partial n} = \left[\dot{Y}(t) + (1 - \beta_1)\Delta t\,\ddot{Y}(t) + \beta_1 \Delta t\,\ddot{Y}(t+1)\right] n_x \qquad \text{on } S_i \quad ; \; i = 1,2,....,N,c,o \tag{9}$$

where the ground acceleration $\ddot{Y}(t+1)$ is known. When the rigid body does slide, the kinematic body surface conditions should be expressed in terms of the velocity potential $\Phi(t+1)$ so as to satisfy the equation of motion shown in Eq. (2). Applying Newmark's integration scheme to the absolute displacement X(t) of the rigid body, the absolute acceleration $\ddot{X}(t+1)$ is given by

$$\ddot{X}(t+1) = \frac{1}{\beta_1 \Delta t}\left[\dot{X}(t+1) - B(t)\right] \qquad ; \qquad B(t) = \dot{X}(t) + (1 - \beta_1)\Delta t\,\ddot{X}(t) \tag{10}$$

Substituting Eq. (10) into the equation of motion given by Eq. (2), and solving it in terms of the absolute velocity $\dot{X}(t+1)$, the following equation is obtained.

$$\dot{X}(t+1) = \frac{\beta_1 \Delta t}{M}\left[-\,\mathrm{sgn}\left[\dot{U}(t+1)\right]\mu_d W' - F(t+1)\right] + B(t) \tag{11}$$

where F(t+1) is the horizontal hydrodynamic restoring force at the time of (t+1), which can be derived by integrating the hydrodynamic pressure over the body surface.

$$F(t+1) = -\rho \sum_{j=1}^{N,c,o} \int_{S_{wj}} n_x \left[\frac{\beta_1}{\beta_2 \Delta t} \Phi_j(t+1) + D_j(t) \right] ds \quad ; \quad D_j(t) = \dot{\Phi}_j(t) + (1-\beta_1)\,\Delta t \ddot{\Phi}_j(t) - \frac{\beta_1}{\beta_2 \Delta t} A_j(t) \qquad (12)$$

where ρ is mass density of fluid. Substituting the horizontal hydrodynamic restoring force expressed by Eq. (12) into Eq. (11), the absolute velocity $\dot{X}(t+1)$ can be expressed in terms of the velocity potential $\Phi(t+1)$. Finally the kinematic body surface boundary conditions which are ready for the boundary integral equation are obtained as follow.

$$\frac{\partial \Phi_i}{\partial n} = n_x \frac{\beta_1 \Delta t}{M} \left[-\mathrm{sgn}(\dot{U}) \mu_d W' + \rho \sum_{j=1}^{N,c,o} \int_{S_{wj}} n_x \left[\frac{\beta_1 \Phi_j(t+1)}{\beta_2 \Delta t} + D_j(t) \right] ds \right] + n_x B(t) \quad \text{on } S_{wi} \; ; i = 1,2,..,N,c,o \qquad (13)$$

The open boundary scheme in this paper follows the extended Orlanski condition proposed by Tanaka and Nakamura (1991). The critical point for this problem is how and where to evaluate the time-dependent behavior of the phase velocity C. The phase velocity at the time of t is determined by

$$C(t) = -\dot{\Phi}_o(t) \Big/ \frac{\partial \Phi_o}{\partial x} \quad ; \quad \dot{\Phi}_o(t) = \frac{\beta_1 \Phi_o(t)}{\beta_2 \Delta t} + D_o(t-1) \qquad (14)$$

where the value $\partial \Phi_o(t)/\partial x$ can be calculated by 4th order numerical backward differentiation on the free surface points

$$\frac{\partial \Phi_o}{\partial x} = \frac{3\Phi_o^{-4} - 16\Phi_o^{-3} + 36\Phi_o^{-2} - 48\Phi_o^{-1} + 25\Phi_o^{0}}{12\Delta x} \quad \text{where} \quad \Phi_o^{-j} = \Phi_o(x_o - \Delta x\, j) \qquad (15)$$

where Δx is the element length on the free surface and x_o is the x-coordinate of the first node from the open boundary. Now the phase velocity C(t) at each time step can be calculated by Eq. (14); thus, the radiation boundary condition becomes as follow.

$$\frac{\partial \Phi_o(t+1)}{\partial n} = -\frac{1}{C(t)} \left[\frac{\beta_1 \Phi_o(t+1)}{\beta_2 \Delta t} + D_o(t) \right] \quad \text{on } S_o \qquad (16)$$

Boundary Integral Equation

Applying Green's second identity to the velocity potential $\Phi(x,z,t)$ and Green's function G(P,Q) over the interior and exterior fluid domain yields

$$\alpha \Phi_i(Q) = \int_{S_i} \left[\frac{\partial \Phi_i(P)}{\partial n} G(P,Q) - \Phi_i(P) \frac{\partial G(P,Q)}{\partial n} \right] dx \quad ; \; i = 1,2,...N,c,o \qquad \text{where} \quad G(P,Q) = -\frac{\ln r}{2\pi} \qquad (17)$$

where P is a point on the boundary, Q can be either a boundary point or an interior point ($\alpha = 2\pi$) and r denotes the distance between the point P and the point Q. If Q is a boundary point, α is the interior angle of the boundary at point Q. Substituting the boundary conditions given by Eqs. (8), (9), (13) and (16) into the integral equation given by Eq. (17), (N+2) simultaneous integral equations in terms of $\Phi(t+1)$ are obtained.

Sliding Criterion and Convergence Method

It is important to precisely determine whether the body is sliding or not sliding, because two different equations should be solved corresponding to the sliding judgment. The criterion equations from non-sliding to sliding, and from sliding to non-sliding are expressed, respectively.

$$\mu_s W' < \left| M\ddot{Y}(t+1) + F(t+1) \right| \quad ; \quad \mu_d W' > \left| M\left[\ddot{Y}(t+1) + \ddot{U}(t) \right] + F(t+1) \right| \qquad (18)$$

where μ_s is the static friction coefficient. The relative velocity $\dot{U}(t+1)$ is still an unknown variable to determine the velocity potential $\Phi(t+1)$. Predictor-corrector method is employed so that the first prediction is done by using $\dot{U}(t)$ instead of $\ddot{U}(t+1)$ and subsequently the correction is done to converge to some relative errors.

EXPERIMENT AND THEORETICAL VERIFICATION

Model Test Arrangement

The experimental arrangement is illustrated in Fig. 2. The rigid body with two interior liquid tanks is made of acrylic fiber plate and both the bottom of the body and the rigid ground are made of stainless steel plate to keep the friction coefficient stable. The absolute acceleration response and the relative displacement of the rigid body to the ground are measured by the acceleration sensors and the laser beam type displacement sensor, respectively. The dynamic motion of the free surface and the hydrodynamic pressure are measured by wave height gauges and pressure sensors.

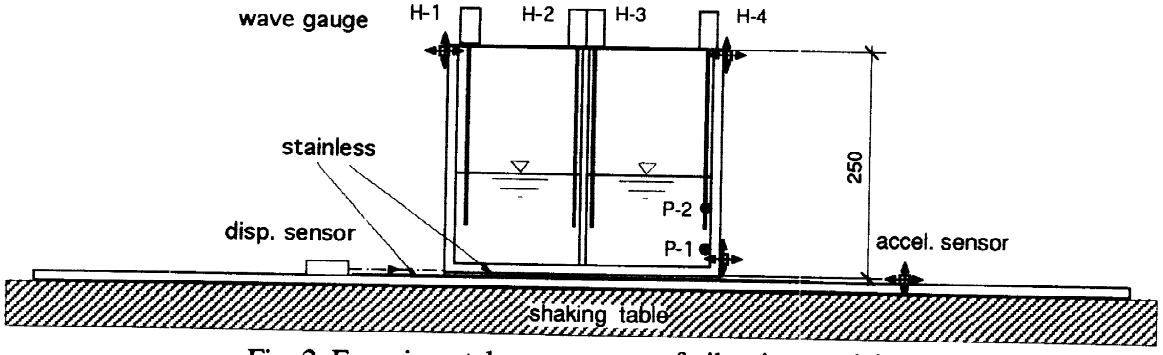

Fig. 2 Experimental arrangement of vibration model test

Test Results and Comparisons

Two cases of experiment have been carried out for Hachinohe earthquake with the maximum acceleration a_m=600 gal; one is without interior fluid but replaced by the equivalent mass of sand and another is with interior fluid of h_i=11 cm in water depth. The comparisons of the experiment and calculation results of the sliding response for the two cases are shown in Fig. 3. The friction coefficients between two stainless plates were estimated from the absolute acceleration sliding response of the body without the interior fluid. It is observed that the relative displacement of the body with interior fluid is smaller than that of the body without interior fluid. The water surface fluctuation of the interior fluid and the hydrodynamic pressure measured in the pressure sensor P-1 are illustrated in Fig. 4. The calculation results demonstrate good agreement with the experimental result. However, the water fluctuation becomes larger, the simulation result gradually becomes discrepant with the laboratory result, because the linearized free surface condition is employed in the theory.

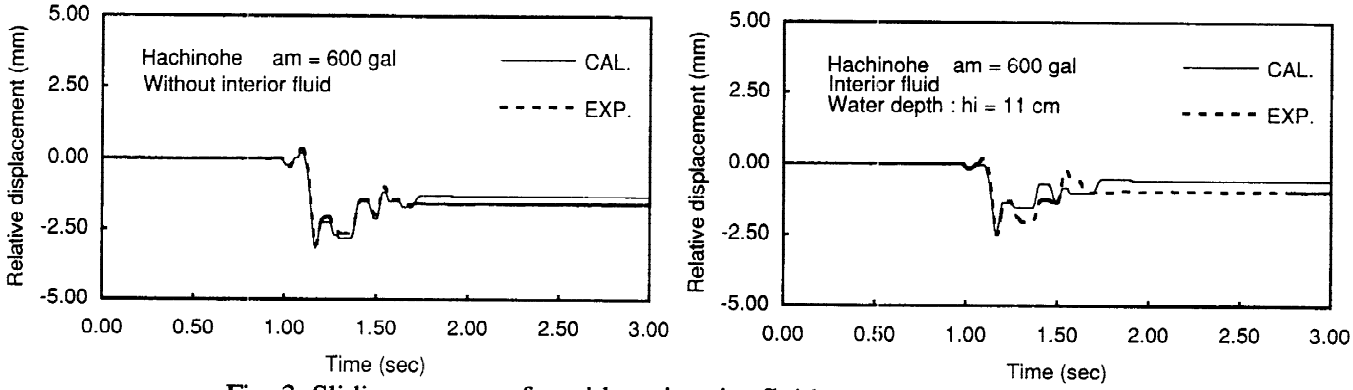

Fig. 3 Sliding response for without interior fluid and with interior fluid

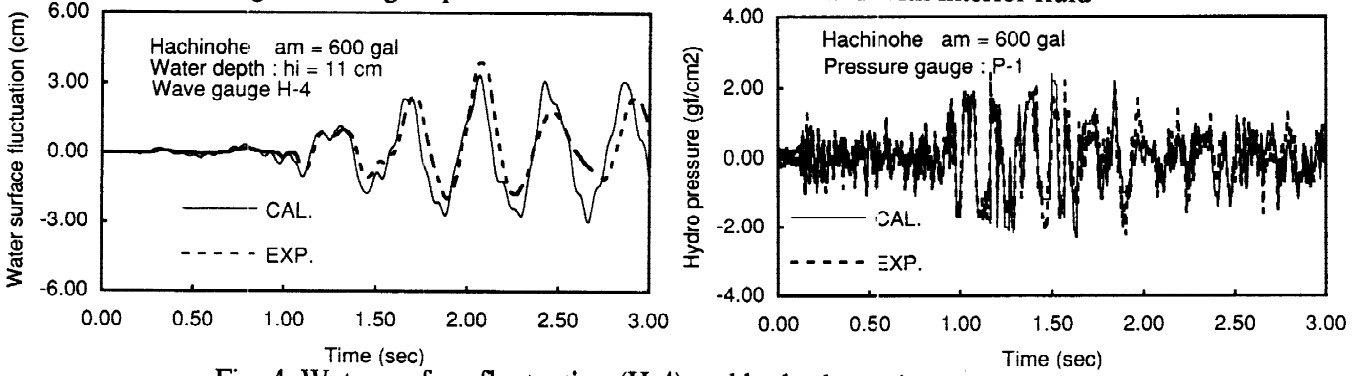

Fig. 4 Water surface fluctuation (H-4) and hydrodynamic pressure (P-1)

NUMERICAL IMPLEMENTATION

Comparison with Westergaard's Solution

If the structure is surrounded by the semi-infinite exterior fluid and it does not slide, then the hydrodynamic restoring pressure on the exterior walls may be predicted by Westergaard's solution which was derived in 1933 for the case of a straight dam. The comparison of the hydrodynamic pressure distributions by Westergaard's analytical solution, his approximate formula and our present method is illustrated in Fig.5a. The calculation condition is that the harmonic ground excitation with frequency f=0.5 Hz and the maximum acceleration amplitude a_0=900 gal for exterior water depth h_e=9.5 m with open boundary L_0=20 m for both side, are forced on the fixed body of the width B=15 m. Westergaard's analytical result is a little larger than our present model which is calculated at the moment t=5.13 sec that the body acceleration is maximum. This is because that Westergaard neglects the generation of the surface waves, while we consider the free surface boundary condition shown in Eq.(3). The free surface elevation at t=5.13 sec coincides with the pressure at the free surface shown in Fig.5b. Westergaard's approximate formula indicates the overestimated pressure values near sea bed and free surface. If the structure is surrounded by open sea, then the simplest modeling of the restoring hydrodynamic force is the application of added mass to the equation of motion. In order to investigate the effect of predicted precision of the restoring force on the sliding response, the added mass model and full coupled present model are compared for the condition shown that a) harmonic ground acceleration with f=2, 5, 10 Hz, a_0=200 gal and b) Hachinohe waves with maximum acceleration a_m=200 gal and $\mu_s=\mu_d$=0.5. The added mass model for both input ground excitations demonstrates larger relative displacement than the present model as shown in Fig. 6, because of the overestimation of Westergaard's approximate formula.

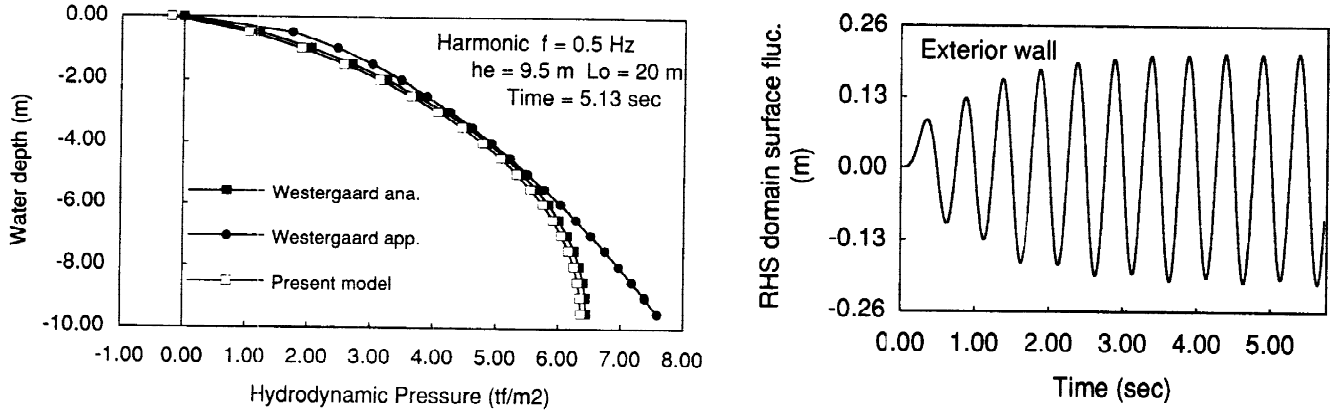

Fig. 5 Hydrodynamic pressure distribution and water surface fluctuation on RHS exterior wall

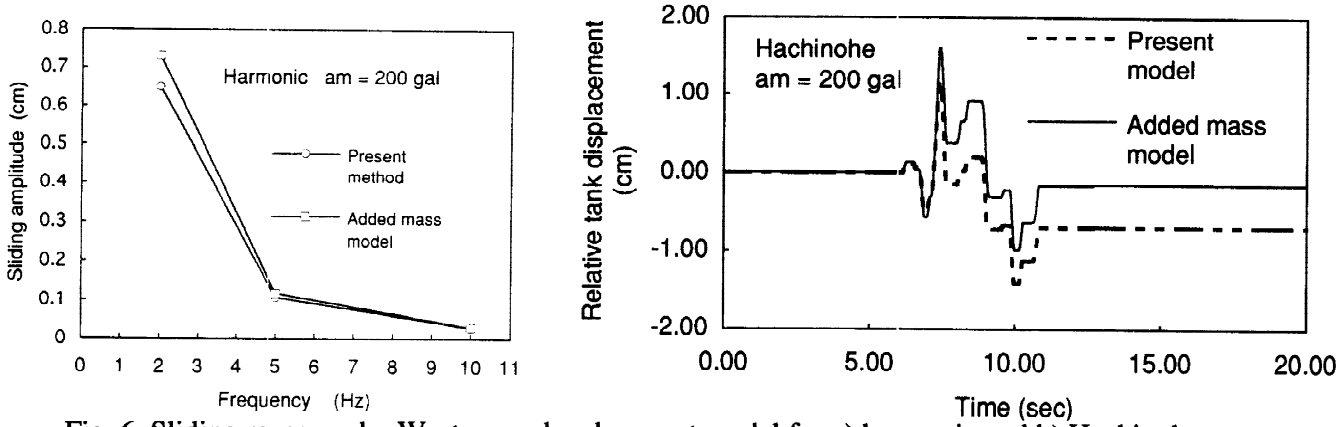

Fig. 6 Sliding response by Westergaard and present model for a) harmonic and b) Hachinohe waves

Effect of Interior Water Depth on Sliding Response

The numerical implementation has been conducted for the condition that the rigid body of B=15 m with two tanks of the water depth h_i=4, 7, 10, 13 m, B_i=6.8 m surrounded by open exterior fluid h_e=9.5 m, L_0=20 m, is excited by the harmonic ground acceleration with f=5 Hz, a_0=200 gal for the friction coefficient $\mu_s=\mu_d$=0.5. The total mass of rigid body and interior fluid M=21.27 ton/m is used even for the different interior water depth. From the calculation result shown in Fig. 7, it is observed that the deeper the interior water depth, the smaller the relative displacement of the body. It is noted that the hydrodynamic restoring forces due to interior fluid motion impose to reduce the sliding amount, therefore the deeper the interior water depth, the larger the restoring hydrodynamic forces act on the interior walls.

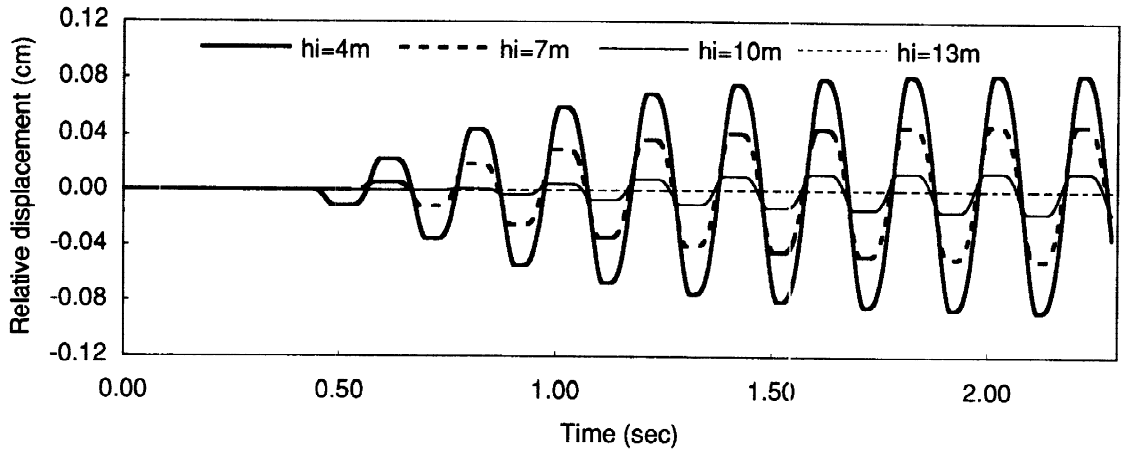

Fig. 7 Sliding response for various interior water depths h_i

Effect of Interior Tank Width on Sliding Response

The water depth of the interior fluid is one parameter to characterize the effects of the interior fluid motion on the sliding response. Another parameter may be the interior tank width. The simulation conditions are exactly same as the interior water depth case in previous section except that the interior water depth is fixed to h_i=7 m and the interior tank width B_i=3.2, 4.4, 6.8, 14 m which corresponds with the interior tank number N_t=4, 3, 2, 1. Figure 8 demonstrates that the relative displacement increase as the interior tank width becomes large (i.e. the number of interior walls decreases). It should be noted that the integrated hydrodynamic restoring forces over the interior fluid domain, which must play an important role to reduce the sliding amount, increase as the number of interior walls increases for the condition of the fixed interior water depth.

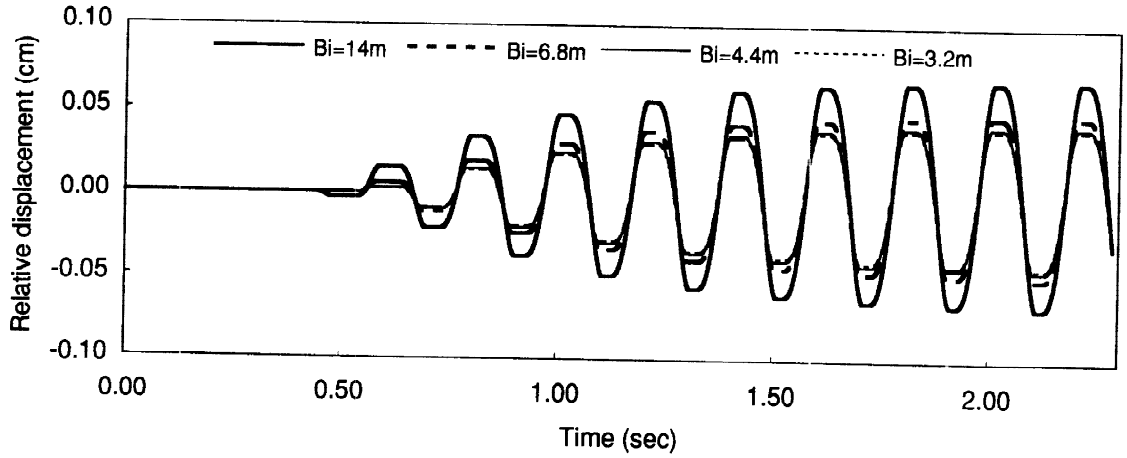

Fig. 8 Sliding response for various interior tank widths B_i

Effect of Side Quay Wall's Location on Sliding Response

In the previous sections the exterior domains of both sides are semi-infinite, namely all propagating waves to the left and right hand side fluid domain must go through both open boundaries where no waves can reflect. If the side quay wall is set to be in the left hand side fluid domain like the definition sketch shown in Fig. 1, the hydrodynamic pressure disturbance and the propagating surface waves from the side quay wall should effect on the sliding response of the structure. The parametric simulations have been conducted for the various lengths L_c=2, 5, 10, 20 m in the left hand side fluid domain. Two interior tanks with h_i=7 m and B_i=6.8 m are set in the structure and the rest of the conditions are same as the previous section. It is observed from the result shown in Fig. 9 that the sliding response of the body decreases as the length L_c. It is reasonable that the hydrodynamic restoring pressures on either side of exterior tank walls may not be symmetric because the fluid motion in left hand side domain is affected by the reflecting waves from the side quay wall. The hydrodynamic pressures on the left and right hand side exterior walls are illustrated at the moment that the body absolute acceleration is maximum and zero, respectively in Fig. 10a and 10b. It should be noted that when the length L_c becomes short, the hydrodynamic pressure tends to reduce compared with the case of open boundary condition and then this reduced restoring force makes it difficult to slide the structure.

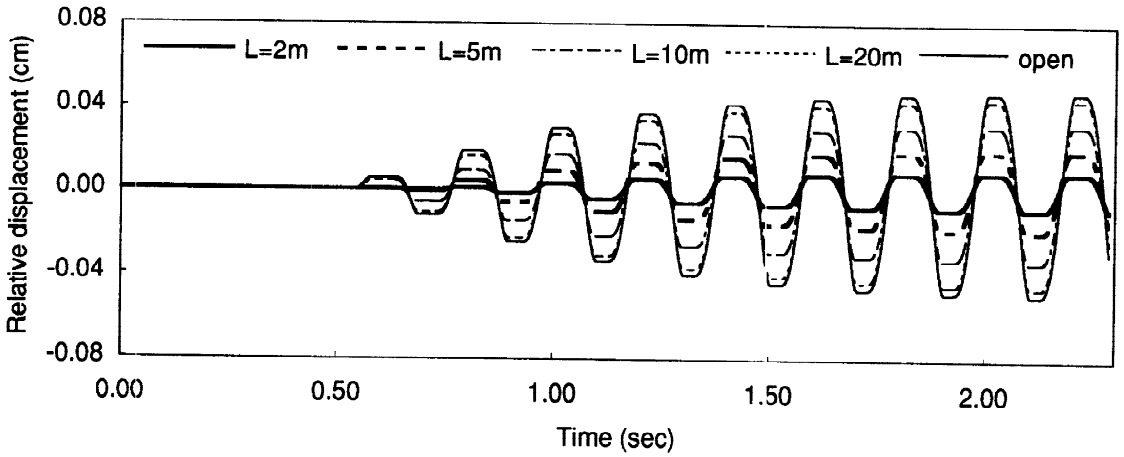

Fig. 9 Sliding response for various lengths L_c=2, 5, 10, 20 m and L_o=20 m in LHS fluid domain

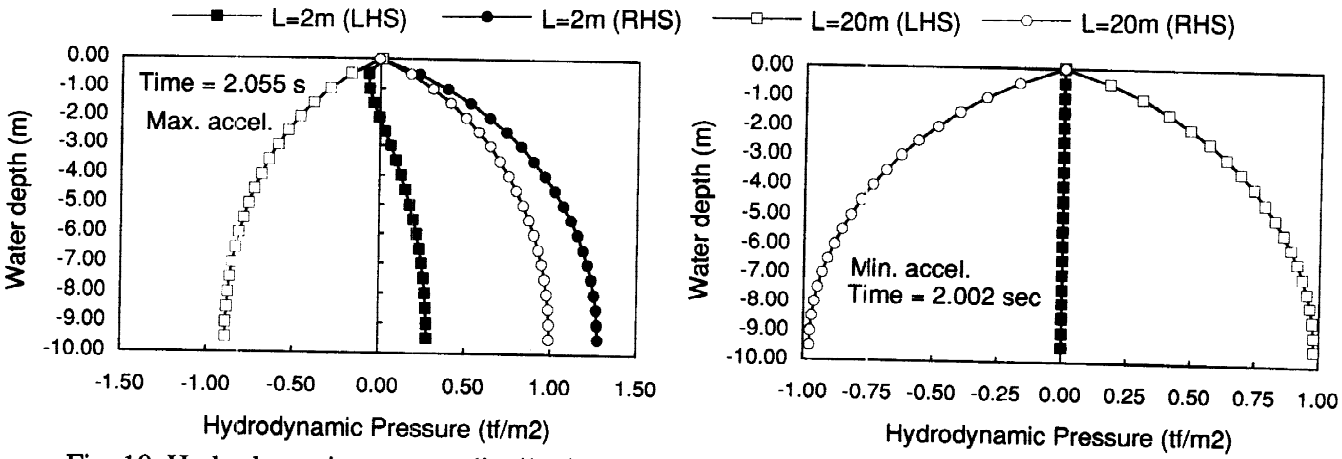

Fig. 10 Hydrodynamic pressure distribution a) in phase and b) out of phase of body acceleration

CONCLUSIONS

1) The hydrodynamic restoring forces of the interior fluid generally act so as to decrease the sliding response.
2) Simplified Westergaard added mass model usually results in the overestimated sliding response.
3) When the structure is surrounded by open sea, the deeper the interior water depth, the smaller the relative displacement of the body for the condition of the same total mass of the body and the liquid.
4) When the structure is surrounded by open sea, the sliding response decreases as the number of interwalls of the storage tank increases for the condition of the fixed interior fluid water depth.
5) As the length between the side quay wall and the exterior body wall becomes short in the finite fluid domain, the restoring force on the exterior wall act so as to reduce the sliding response.

REFERENCES

Fujii, S., M. Iwano, F. Tanizawa and M. Muramatsu (1986). A study of earthquake sliding response. *Proc. the 7th Japan Earthquake Eng. Symp.*, 1075-1080. in Japanese

Orlanski, I. (1976). A simple boundary condition for unbounded hyperbolic flows. *J. Computational Physics., 21*, 251-269.

Tanaka, Y. and R. T. Hudspeth (1988). Restoring forces of vertical circular cylinder. *J. Earthquake Eng. and Struct. Dyn., 16(1)*, 99-119.

Tanaka, Y. and T. Nakamura (1991). Numerical generation of gravity waves and open boundary scheme. *Proc. the 10th Int. Conf. on Offshore Mech. and Arc. Eng.*, 229-235.

Uwabe, T. and N. Higaki (1984). Experimental study of sliding behavior and hydrodynamic pressure of offshore rigid structure due to earthquake. *Report Habor Res. Inst., 23(3)*, in Japanese

Westergaard, H. M. (1933). Water pressure on dams during earthquakes. *Trans. ASCE*, 418-434.

Williams, A. N. (1991). Analysis of the base-excited response of intake-outlet towers by a Green's function approach. *J. Eng. Struct., 13(1)*, 43-53.